Title Page:

Article Title: Evolutionary constraints mediate extinction risk under climate change

Authors: Guillermo Garcia-Costoya[1], Claire E. Williams[1], Trevor M. Faske[1], Jacob D. Moorman[2], Michael L. Logan[1].

Author e-mails (same order): guille@nevada.unr.edu, williams.claire.e@gmail.com, tfaske@nevada.unr.edu, jacob@moorman.me, michaellogan@unr.edu

Affiliations: [1]University of Nevada, Reno, Reno, NV, USA, [2]University of California, Los Angeles, CA, USA

Running title: Evolutionary constraints and climate change

Keywords: genetic correlation, thermal physiology, climate change, evolutionary constraint, extinction risk.

Type of article: Letter

Abstract word count: 144

Main text word count: 4396

Number of figures: 3

Number of references: 65

Corresponding author: Guillermo Garcia-Costoya, **guille@nevada.unr.edu**, +1 (775) 247-4284

Statement of authorship: GGC and MLL conceptualized the project. GGC, TMF, CEW and JDM developed the simulation code, GGC wrote the first draft of the manuscript and all authors contributed to manuscript revision.

Data accessibility statement: All scripts used for this manuscript are available on GitHub at: https://github.com/ggcostoya/tpc_genetic_correlations.

The original data for populations, climate change scenarios and simulation outcomes are stored temporarily on Google Drive at: https://drive.google.com/drive/folders/1nxoNiDcqxyInwjXeWqUe5b4KYCWmzzBf?usp=sharing. Metadata and links to these files are also available through the GitHub repository and upon publication of the manuscript they will be made available and archived in an appropriate public repository.

Abstract:

Mounting evidence suggests that rapid evolutionary adaptation may rescue some organisms from the impacts of climate change. However, evolutionary constraints might hinder this process, especially when different aspects of environmental change generate antagonistic selection on genetically correlated traits. Here, we use individual-based simulations to explore how genetic correlations underlying the thermal physiology of ectotherms might influence their responses to the two major components of climate change—increases in mean temperature and thermal variability. We found that genetic correlations can influence population dynamics under climate change, with declines in population size varying three-fold depending on the type of correlation present. Surprisingly, populations whose thermal performance curves were constrained by genetic correlations often declined less rapidly than unconstrained populations. Our results suggest that accurate forecasts of the impact of climate change on ectotherms will require an understanding of the genetic architecture of the traits under selection.

Main Body:

Introduction

Global climate change is a major threat to life on Earth, with climate models predicting continued increases in both the mean and variability of environmental temperature (Allan et al., 2021; Bathiany et al., 2018). Ongoing shifts in thermal environments have already been linked to negative impacts on organisms and have resulted in dramatic declines in many taxonomic groups (Bellard et al., 2012; Sinervo et al., 2010). As climate change progresses, organisms must respond to these pressures in order to persist. Organismal responses can occur in various ways, including range shifts (Booth et al., 2011; Elmhagen et al., 2015), behavioral or phenological modifications (Fey et al., 2019; Kearney et al., 2009), or acclimatization (Charmantier et al., 2008; Cohen et al., 2018; Ovaskainen et al., 2013). Nonetheless, species for which these mechanisms are insufficient (e.g., species with limited dispersal capacity) must rely on *in situ* genetic adaptation to survive (Hairston et al., 2005; Hoffmann & Sgrò, 2011).

A range of intrinsic and extrinsic variables determine the ability of populations to evolve rapidly in the face of shifting thermal environments. First, the opportunity for natural selection is limited by the amount of phenotypic diversity within a population, while the efficacy of selection (i.e., the evolutionary response) is mediated by the heritability and genetic architecture of the relevant traits (Fisher, 1958). Large populations typically have greater levels of both phenotypic and genetic variation, and they have more individuals by which to resist selection load — the increased mortality and drop in population size that can arise from strong selection (Frankham, 1996; Lande, 1993). Nonetheless, even in large populations, traits may be genetically correlated in ways that either enhance or constrain the response to selection (Chevin, 2013; Kingsolver & Diamond, 2015; Logan & Cox, 2020; Schou et al., 2022). Thus, genetic

correlations may impact population dynamics as environments change, but this possibility has largely been overlooked in the climate-impact literature.

Genetic correlations are the result of relationships between traits at the genetic level and can arise through ultimate (evolutionary) mechanisms like correlational selection (Roff & Fairbairn, 2012) and proximate (developmental) mechanisms like pleiotropy or linkage disequilibrium (Hochachka & Somero, 2002). Genetic correlations result in limitations to the space and direction along which phenotypes vary in a population (Chevin, 2013). Consequently, identifying how genetic correlations mediate rapid evolutionary change in climate-related traits is crucial for accurately predicting organismal responses to climate change. Indeed, because climate change represents at least two distinct axis of environmental change (increasing mean and variance of environmental temperature) that serve as agents of selection on different traits, genetic correlations among these traits may play a disproportionate role in the dynamics of adaptation (Logan & Cox, 2020).

Climate forecasts project that mean environmental temperature will increase globally between 1 and 3°C by the end of the 21st century (Allan et al., 2021). A similar pattern has been predicted for thermal variability, with an expected 15% increase in standard deviation for every 1°C increase in mean temperature (Bathiany et al., 2018). These changes may be especially profound for ectotherms due to their inability to regulate internal body temperature using physiological means. The primary traits that dictate an ectotherm's relationship with its thermal environment are those that underly the thermal performance curve (TPC). For ectotherms, TPCs are functions that describe the relationship between body temperature to performance or fitness (Angilletta, 2009; Huey & Stevenson, 1979), and the parameters of these curves can be considered traits that combine to describe their shape. The thermal optimum (T_{opt}) is the body

temperature where maximum performance (P_{max}) is achieved. The critical thermal minimum (CT_{min}) and maximum (CT_{max}) are known as the critical thermal limits and are the body temperatures where performance drops to zero. The critical thermal limits, along with the magnitude of increase and decrease in performance with increasing temperature below and above T_{opt}, respectively, jointly determine the breadth of the TPC (T_{br}; Figure 1A). An increase in mean environmental temperature should select for an increase in T_{opt} (Logan et al., 2014), whereas an increase in thermal variability should select for lower CT_{min}, higher CT_{max}, and a wider T_{br} (Gilchrist, 1995). Thus, in the absence of constraints, climate change should result in the evolution of broader TPCs with higher thermal optima.

Nevertheless, two major categories of genetic correlations that constrain TPC shapes have been identified in natural populations of ectotherms. These are the "generalist-specialist trade-off" (GSTO) and the "thermodynamic effect" (TDE; also known as the "hotter-is-better" hypothesis). A GSTO is present when the area under the TPC remains constant despite shifts in TPC shape (Figure 1B), and this pattern has been observed in many species at the phenotypic level (Condon et al., 2015; Gilchrist, 1996; Gilchrist et al., 1997; Kingsolver et al., 2015; Latimer et al., 2011; Phillips et al., 2014; Richter-Boix et al., 2015). Aspects of the GSTO, including negative correlations between CT_{min} and CT_{max} or between P_{max} and T_{br} have also been documented at the genetic level in some species (Berger et al., 2014; Izem & Kingsolver, 2005; Kingsolver et al., 2004; Knies et al., 2006). The GSTO is thought to occur because of the antagonistic pleiotropy that arises from the cost imposed by maximizing performance in the local thermal environment (i.e., "a jack of all environments is a master of none"; Gilchrist, 1996). A TDE is present when there is a positive correlation between T_{opt} and P_{max} (Figure 1C). As with the GSTO, the TDE has been observed at both the phenotypic (Knies et al., 2009; Phillips et al.,

2014) and genetic (Bennett et al., 1992; Berger et al., 2014) levels and is thought to arise because biochemical reaction rates are more efficient at warmer temperatures (Angilletta et al., 2010). Furthermore, growing evidence suggests that both the GSTO and TDE can occur within the same population (Gilchrist, 1996; Logan et al., 2018; Logan & Cox, 2020; Martins et al., 2019; Figure 1D) raising the possibility that some populations might be able to adapt to either rising mean temperatures or increasing thermal variability, but not both (Logan et al., 2020; Logan & Cox, 2020). These types of genetic correlations may be ubiquitous in natural populations and could have important effects on the evolutionary potential of ectotherms under climate change.

Here, we examined the role of genetic correlations in the responses of ectotherms to multidimensional climate change using individual-based simulations. First, we generated a set of populations of ectotherms differing in the genetic correlations constraining their TPC shapes and in initial population size. Then, we exposed them to climate change scenarios of varying magnitudes following IPCC predictions, tracking trait evolution and changes in population size over 80 generations. We hypothesized that genetic correlations would affect extinction probabilities in a rank-order fashion in the following way: 1) populations whose TPCs were constrained only by the TDE would fare the best, followed by 2) populations with no genetic correlations at all, 3) populations that were constrained only by the GSTO, and finally, 4) populations constrained by both the TDE and the GSTO. We also hypothesized that extinction would occur fastest in populations with the smallest initial size, but that the relative vulnerability of populations exposed to a given set of genetic constraints would be consistent irrespective of starting population size. Our analysis represents, to our knowledge, the first attempt to simulate the role of genetic constraints on rapid adaptation and extinction risk under contemporary

147 climate change and has important implications for understanding the vulnerability of ectotherms
148 to rapid environmental change.
149
150 **Methods**
151 To examine the role of genetic correlations in the responses of ectotherms to climate change, we
152 conducted individual-based simulations that challenged populations of a hypothetical
153 ectothermic animal with increasingly warmer and variable thermal environments. Each
154 individual was defined exclusively by their thermal performance curve (TPC), making the match
155 between the shape of their TPC and the environmental temperature the sole determinant of their
156 performance and ultimately their survival and reproduction. For some simulations, we introduced
157 genetic correlations that limited the possible range of shapes that TPCs within a population could
158 assume.
159 We considered a hypothetical ectotherm species that, like many insects and small
160 vertebrates, had an annual reproductive cycle with non-overlapping generations. Our organism
161 reproduced asexually via perfect cloning (i.e., the narrow-sense heritability of TPC parameters
162 was 1). We did not allow mutation to occur, as theoretical and empirical work has demonstrated
163 that the majority of adaptive evolution over short timescales occurs via changes in standing
164 genetic variation (Barrett & Schluter, 2008; Burke et al., 2014; Chaturvedi et al., 2021;
165 Schlötterer et al., 2015; Teotónio et al., 2009). Our hypothetical ectotherm was a
166 thermoconformer, meaning that the environmental temperatures they experienced were
167 equivalent to their body temperatures. Lastly, populations evolved in a closed environment (i.e.,
168 no gene flow) that was thermally homogeneous in space. We generated 120 unique starting
169 populations whose TPCs were subject to one of four genetic correlation scenarios: 1) no genetic

correlations, 2) generalist-specialist trade-off (GSTO), 3) thermodynamic effect (TDE), and 3) both a specialist-generalist trade-off and a thermodynamic effect (GSTO + TDE; Figure 1). Within each genetic correlation scenario, we ran simulations with three different initial population sizes (N_0 = 50, N_0 = 500 & N_0 = 5000), and we set carrying capacity (K) equal to N_0. After allowing acclimatization to an initially stable environment for five generations, populations were exposed to changing thermal regimes for 80 generations (through the end of the century), following the global average predictions of the three main IPCC climate change scenarios: RCP 4.5, RCP 6, and RCP 8.5 (IPCC 2021, Allan et al., 2021). In this primary set of simulations, both the mean and variability of temperature increased simultaneously following climate forecasts. We further isolated the role of changing mean temperature versus changing thermal variability by conducting an additional set of simulations where we allowed only the mean or the variability to change. As each simulation unfolded, we recorded changes in population size, extinction rate, and the evolution of TPCs.

Further details on the processes of generating the starting populations, simulating thermal environments, and the modelling of survival and reproduction, can be found in the supplementary materials. All code for this manuscript was written using the R language (R Core Team 2021). Simulations were run on a high-performance computing cluster at the University of Nevada, Reno.

Results

Our hypothetical ectotherm populations were able to withstand the two least severe climate change scenarios, irrespective of the genetic correlations present (RCP 4.5 and RCP 6). On average, with respect to the initial size and across all simulations challenged with a particular

climate change scenario, population sizes decreased by only 3% and 6% for the RCP 4.5 and RCP 6 scenario. These declines were similar to the control scenario where no environmental change occurred and average population size did not decrease at all (Figure 2, Figure S1A, Table S1). Nonetheless, for the more severe RCP 8.5 scenario, population size decreased on average by 56%, indicating a much higher likelihood of extinction if climate change progresses via this worst-case scenario (Figure 2, Table S1).

Changes in mean and/or standard deviation also produced different patterns of population decline. For the RCP 8.5 scenario, when we allowed only mean temperature (Figure S1D) or thermal variability (Figure S1E) to change, increases in mean temperature (average decline of 19%) were more detrimental than increases in standard deviation (no decline). When further exploring the influence of thermal variability, we saw that a more variable initial thermal environment (initial T_{sd} = 2°C instead of 1°C), but with no changes in thermal conditions over time, led to frequent fluctuations in population size by the end of the simulation, indicating that populations were maladapted to starting conditions but were able to persist by adapting over time (Figure S1B). If we allowed thermal conditions to change following the RCP 8.5 scenario, an initially more thermally variable environment always resulted in extinction by the 80^{th} generation of change (Figure S1C).

Unsurprisingly, initial population size played an important role in mediating extinction risk. Populations of N_0 = 50 declined by an average of 37% after 80 generations of change (across all scenarios excluding the control; Figure 2A-C, Table S1). In contrast, populations of N_0 = 500 and N_0 = 5000 declined by an average of 15% and 13%, respectively (Figure 2D-I, Table S1).

Genetic correlations played an important role in determining the extent of population decline. Populations subject to the GSTO experienced the most severe population size declines (average decline of 35%) closely followed by populations subject to no genetic correlations at all (average decline of 33%). Populations subject to the TDE performed best, only declining by an average of 11%. Populations subject to both the GSTO and the TDE declined by an average of 17% (Figure 2, Table S1). Despite notable differences in population decline depending on the type of genetic constraint present, all populations followed similar trajectories with respect to changes in average reproductive success, regardless of the particular combination of climate change scenario and genetic constraint. Mean reproductive success increased in early stages (generations 0-20) but then declined continuously until the end of the simulation with varying degrees of intensity depending on the genetic constraints present and the climate change scenario (Figure 3A, S3A, S4A).

As expected, TPC shape evolved in response to environmental change. By the end of our simulations, CT_{min}, T_{opt}, CT_{max} and P_{max} had increased by an average of 0.6 °C, 1.8 °C, 0.25 °C, and 2.23, and by 0.6 °C, 2.1 °C, 0.7 °C, and 2.15 for the worst climate change scenario we considered (RCP 8.5, Table S3). Initially, TPCs with high values of both P_{max} and T_{opt} were favored by selection across all simulations. However, the particular set of genetic correlations present in a given set of simulations affected the ability of populations to achieve local fitness optima. For example, in the initial generations, GSTO + TDE constrained populations achieved the highest values of P_{max}, whereas populations subjected to only the TDE achieved the highest values of T_{opt}. Populations whose TPCs were unconstrained by genetic correlations achieved comparatively low values of both of these traits in the early stages of the simulation. Additionally, the relationships between traits imposed by genetic correlations resulted in the

correlated evolution of these traits. For GSTO and GSTO + TDE constrained populations, CT_{min} and CT_{max} increased and decreased, respectively, due to the loss in thermal breath associated with gains in P_{max}. In contrast, the TPCs of populations that were unconstrained by genetic correlations evolved to be broader. In other words, unconstrained populations evolved towards generalism (lower CT_{min} and higher CT_{max}) as the simulation unfolded (Figure 3B-D, S3B-D, S4B-D, Table S3).

Discussion

As climate change progresses, organisms will be faced with novel selection pressures that might require *in situ* adaptation (Hairston et al., 2005; Hoffmann & Sgrò, 2011). However, the potential for evolutionary rescue depends on several factors, including the presence and structure of genotypic and phenotypic variation (Chevin, 2013; Kingsolver & Diamond, 2015). Genetic correlations, which are known to occur between traits that underly the thermal performance curves of ectotherms, might influence evolutionary (and therefore, population) responses, but the ways in which this might occur have not been previously tested. Our simulations revealed that evolutionary constraints in the form of genetic correlations might influence the ability of ectotherms to adapt to climate change, especially when the rate of change in thermal environments is high. Surprisingly, and in disagreement with our *a priori* hypotheses, genetic correlations often increased adaptive potential. Finally, we found that the specific ways in which thermal environments shifted (i.e., changing mean temperature versus thermal variability) had strong effects on extinction probabilities.

There is ample empirical evidence that TPCs of wild organisms are subject to phenotypic correlations that follow the GSTO and TDE. While the mechanisms that underly these

phenotype-level patterns are less clear, growing evidence suggests that genetic correlations are at play in at least some cases (Angilletta et al., 2010; Berger et al., 2014; Condon et al., 2015; Gilchrist, 1996; Gilchrist et al., 1997; Izem & Kingsolver, 2005; Kingsolver et al., 2004, 2015; Knies et al., 2006, 2009; Latimer et al., 2011). A few studies have even presented evidence of both the GSTO and TDE occurring at the genetic level in the same population (Logan et al., 2020; Martins et al., 2019). In our study, we hypothesized that the limitations on phenotypic variability caused by genetic correlations like the TDE could be beneficial in adapting to climate change while others like the GSTO might be detrimental. We also hypothesized that the combination of these two types of genetic correlation would be the most harmful, leading to the rapid evolution of specialization (increasing T_{opt} leading to increasing P_{max} which in turn leads to decreasing T_{br}) followed by population extinction in later stages when thermal environments become highly variable. Finally, we hypothesized that unconstrained TPC evolution (the complete absence of genetic correlations) would decrease the likelihood of extinction compared to every genetic correlation scenario except for the TDE.

With respect to populations constrained by either the TDE or the GSTO, our simulations predicted outcomes similar to what we had hypothesized. Populations subjected to the TDE declined the least across all climate change scenarios whereas the GSTO-constrained populations declined the most (Figure 2). Among populations subjected to the TDE and no other genetic correlation, the initial environment favored individuals with high P_{max} that, due to the genetic correlation, also had higher T_{opt} (Figure 3, Figure S2H). In early stages of environmental change, this correlation between traits decreased the degree of overlap between the populations' average TPC and the distribution of environmental temperatures leading to lower reproductive success. Nonetheless, the initial increase in T_{opt} produced TDE populations that were pre-adapted to the

much warmer environment that would emerge in later generations (Figure 3C). Our results agree with previous studies which suggest that the gains in performance offered by the TDE (e.g., through increased reproductive or developmental rates; Walters et al. 2012), might offer some ectotherms an advantage in the face of climatic change (Angilletta et al. 2010, Walters et al. 2012, Logan & Cox 2020).

Among populations subject to the GSTO and no other genetic correlation, natural selection also favored high P_{max} phenotypes before substantial environmental change had occurred, however, this had a two-fold negative impact. First, due to the GSTO, individuals with high P_{max} values that were favored in early generations had reduced TPC breadth which left them vulnerable to increasing thermal variability. Second, individuals with T_{opt} values matching the mean temperature of the starting thermal environment were heavily favored, leading to an early loss of heat-adapted individuals. These two circumstances ultimately led to the rapid evolution of "cold-adapted" specialists (i.e., adapted to the historically cooler thermal environment) and made GSTO-constrained populations susceptible to increases in both mean temperature and thermal variability (Figure 3). The GSTO is by far the most common genetic constraint found in ectotherm populations (Logan et al. 2020), and thus may represent an important driver of extinction risk in nature.

Populations subject to both the GSTO and TDE, as well as those subjected to no genetic correlations at all, did not follow our *a priori* hypotheses. For example, when populations were constrained by both types of correlations, they did better than when they were only constrained by the GSTO, suggesting that the adaptive benefits conferred by the TDE might outweigh the limitations imposed by the GSTO (Figure 2). As previously mentioned, the GSTO promoted an increase in P_{max} and a decrease in TPC breath during the early stages of adaptation. Nonetheless,

307 the presence of the TDE palliated the effects of maladaptation to warmer environments by
308 forcing high P_{max} individuals to also have higher T_{opt}. In other words, when both genetic
309 correlations are present, heat-adapted individuals are retained in early generations (Figure 3).
310 Surprisingly, populations that were unconstrained by genetic correlations fared worse
311 than almost any set of populations where genetic correlations were present (unconstrained
312 populations performed similarly to those subject to the GSTO; Figure 2). The comparatively high
313 extinction likelihood of genetically unconstrained populations was due to the absence of
314 mechanisms allowing the existence of phenotypes with enhanced performance and reproductive
315 success in the earlier stages of the simulation (Figure 3, Figure S2A-C). Compared to
316 unconstrained populations, GSTO-constrained populations experienced enhanced reproductive
317 output at the beginning of simulations because the specialist individuals that were favored by
318 selection also had higher maximal performance (Figure 3). This increase in early reproductive
319 capacity among GSTO-constrained populations ultimately led to similar extinction probabilities
320 of GSTO-constrained and unconstrained populations even though the former populations
321 declined faster during the later stages of the simulations (Figure 2). This result highlights the role
322 of early local adaptation influencing longer term extinction probabilities via effects on
323 population size and highlights the fact that genetic correlations can be benign or even beneficial.
324 It is important to note, however, that GSTO-constrained populations did worse than
325 unconstrained populations when we doubled thermal variability at the start of simulations
326 (Figure S1C), indicating that selection for broader TPCs in these highly variable thermal
327 environments resulted in heavily reduced maximal performance capacity that prevented
328 evolutionary rescue.

What are the respective roles of changing mean temperature versus increasing thermal variability in driving extinction risk? We explored this question by running a set of simulations where either mean temperature or thermal variability was allowed to increase while the other variable remained constant. Changes in thermal variability alone did not have negative impacts on any of our populations (Figure S1D). On the other hand, changes in mean temperature did have a negative impact, but only on those populations subjected to the GSTO or to no genetic correlations at all (Figure S1E). Our results suggest that ectotherms with some genetic architectures may be more limited by an ability to adapt to warmer environments than to more variable ones. While previous studies have suggested that increasing thermal variability will play an important role in driving population decline (Clusella-Trullas et al., 2011; Deutsch et al., 2008; Vasseur et al., 2014), our simulations suggest that it is the synergistic effects of both increasing mean temperature and thermal variability, rather than either on their own, that will most profoundly influence extinction risk. With that said, we also note that thermal variability played a much stronger role when the initial environment started out more thermally variable. It was these simulations in which all populations went extinct, regardless of whether they were constrained by genetic correlations (Figure S1C).

As we hypothesized, our simulations showed that larger population sizes and carrying capacities reduced extinction probabilities (Figure 2). For any given set of genetic correlations, starting population size interacted with the rate of climate change to determine the relative vulnerability of populations. For starting populations sizes of 50, a large percentage of populations went extinct by 2100, whereas many fewer went extinct when the starting population size was 500 or 5000. Population size plays a dominant role in maintaining genetic and phenotypic variation and is often considered the most important predictor of extinction risk in

changing environments (O'Grady et al., 2004). The greater phenotypic variation afforded by higher population size increases the opportunity for selection and decreases the risk posed by stochastic events (Fisher, 1958; Frankham, 1996; Lande, 1993).

Our analyses have several caveats that must be considered when attempting to extrapolate our results to real world systems. First, our hypothetical ectotherm populations were modeled as populations of TPCs. In real populations, TPC traits might correlate or trade-off with other traits that themselves may be under selection as climate change progresses. In other words, there are potentially many other relevant genetic correlations interacting with complex selection surfaces that we did not consider in this study. For example, individuals with higher values of T_{opt} might also be bolder, and if bolder individuals are more susceptible to predation, negative selection on boldness might counteract the positive selection on T_{opt}, leading to zero evolutionary change in either trait and generating different extinction probabilities from the ones presented here. Future empirical and theoretical studies would benefit from considering these sorts of "complex phenotypes" and how they may affect population dynamics in changing environments. Second, our populations evolved in a spatially homogeneous thermal environment. While many ectotherms live in these kinds of environments (e.g., tropical forest species; Logan et al., 2021; Neel et al., 2021) and therefore thermoconform, many others live in spatially heterogenous thermal environments that permit behavioral thermoregulation (Sears et al., 2016; Sears & Angilletta, 2015). Behavioral thermoregulation is likely to reduce the strength of selection on TPCs (a phenomenon termed the 'Bogert Effect'; Huey et al., 2003, Logan et al., 2019, Muñoz, 2022) while reducing population decline, at least during earlier periods of environmental change (Buckley et al., 2015). Simulations that examine population dynamics and the evolution of TPCs in spatially heterogenous environments where individuals are allowed to thermoregulate are

likely to be informative. Third, our populations reproduced clonally with perfect heritability (i.e., genotypes and phenotypes were identical). Yet variation in most traits is driven, at least in part, by local environmental effects. As with behavioral thermoregulation, plasticity in TPCs might shield organisms from selection as climate change progresses but it could ultimately facilitate adaptation via genetic accommodation (Chevin et al., 2013). The role of plasticity in genetic evolution and population dynamics in changing environments is a rapidly growing area of research (Fox et al., 2019), and future simulations could explore these dynamics by defining a set of reaction norms that are applied to populations of TPCs experiencing changing thermal environments. Despite these important caveats, our simulations provide a deep first attempt and understanding the role of genetic correlations in the vulnerability of ectotherms to climate change.

Through individual-based simulations, we showed that extinction risk under rapid climate change may be mediated by several types of genetic correlations that are frequently observed to underly the thermal performance curves of real populations. Further, these genetic correlations usually enhanced survival relative to populations that are unconstrained by genetic correlations, and the magnitude of these beneficial effects depend on the specific nature of environmental change. Although recent studies have emphasized the importance of changing thermal variability in generating extinction risk, our simulations suggest that increases in thermal variability on their own may have little impact, but instead act synergistically with increasing mean temperatures to threaten organisms. In summary, our results highlight the importance of treating climate change as multi-dimensional and considering the genetic architecture of the traits under selection when predicting extinction risk.

Acknowledgements

We thank Lutz Fromhage, Eric Riddell, Christian Cox, Jennifer Heppner, José F. García-Martínez and the EvolDoers discussion group at the University of Nevada Reno for helpful comments on the manuscript.

References

Allan, R. P., Hawkins, E., Bellouin, N., & Collins, B. (2021). *IPCC, 2021: Summary for Policymakers* (V. Masson-Delmotte, P. Zhai, A. Pirani, S. L. Connors, C. Péan, S. Berger, N. Caud, Y. Chen, L. Goldfarb, M. I. Gomis, M. Huang, K. Leitzell, E. Lonnoy, J. B. R. Matthews, T. K. Maycock, T. Waterfield, O. Yelekçi, R. Yu, & B. Zhou, Eds.; pp. 3–32). Cambridge University Press. https://centaur.reading.ac.uk/101317/

Angilletta, M. J. (2006). Estimating and comparing thermal performance curves. *Journal of Thermal Biology*, *31*(7), 541–545. https://doi.org/10.1016/j.jtherbio.2006.06.002

Angilletta, M. J. (2009). *Thermal Adaptation: A Theoretical and Empirical Synthesis*. OUP Oxford.

Angilletta, M. J., Huey, R. B., & Frazier, M. R. (2010). Thermodynamic Effects on Organismal Performance: Is Hotter Better? *Physiological and Biochemical Zoology*, *83*(2), 197–206. https://doi.org/10.1086/648567

Barrett, R. D. H., & Schluter, D. (2008). Adaptation from standing genetic variation. *Trends in Ecology & Evolution*, *23*(1), 38–44. https://doi.org/10.1016/j.tree.2007.09.008

Bathiany, S., Dakos, V., Scheffer, M., & Lenton, T. M. (2018). Climate models predict increasing temperature variability in poor countries. *Science Advances*. https://doi.org/10.1126/sciadv.aar5809

Bellard, C., Bertelsmeier, C., Leadley, P., Thuiller, W., & Courchamp, F. (2012). Impacts of climate change on the future of biodiversity. *Ecology Letters*, *15*(4), 365–377. https://doi.org/10.1111/j.1461-0248.2011.01736.x

Bennett, A. F., Lenski, R. E., & Mittler, J. E. (1992). Evolutionary Adaptation to Temperature. I. Fitness Responses of Escherichia Coli to Changes in Its Thermal Environment. *Evolution*, *46*(1), 16–30. https://doi.org/10.1111/j.1558-5646.1992.tb01981.x

Berger, D., Walters, R. J., & Blanckenhorn, W. U. (2014). Experimental evolution for generalists and specialists reveals multivariate genetic constraints on thermal reaction norms. *Journal of Evolutionary Biology*, *27*(9), 1975–1989. https://doi.org/10.1111/jeb.12452

Booth, D. J., Bond, N., Macreadie, P., Booth, D. J., Bond, N., & Macreadie, P. (2011). Detecting range shifts among Australian fishes in response to climate change. *Marine and Freshwater Research*, *62*(9), 1027–1042. https://doi.org/10.1071/MF10270

Buckley, L. B., Ehrenberger, J. C., & Angilletta, M. J. (2015). Thermoregulatory behaviour limits local adaptation of thermal niches and confers sensitivity to climate change. *Functional Ecology*, *29*(8), 1038–1047.

Burke, M. K., Liti, G., & Long, A. D. (2014). Standing Genetic Variation Drives Repeatable Experimental Evolution in Outcrossing Populations of Saccharomyces cerevisiae. *Molecular Biology and Evolution*, *31*(12), 3228–3239. https://doi.org/10.1093/molbev/msu256

Chaturvedi, A., Zhou, J., Raeymaekers, J. A. M., Czypionka, T., Orsini, L., Jackson, C. E., Spanier, K. I., Shaw, J. R., Colbourne, J. K., & De Meester, L. (2021). Extensive standing genetic variation from a small number of founders enables rapid adaptation in Daphnia. *Nature Communications*, *12*(1), 4306. https://doi.org/10.1038/s41467-021-24581-z

444 Chevin, L.-M. (2013). Genetic Constraints on Adaptation to a Changing Environment. *Evolution*,
445 *67*(3), 708–721. https://doi.org/10.1111/j.1558-5646.2012.01809.x
446 Chevin, L.-M., Collins, S., & Lefèvre, F. (2013). Phenotypic plasticity and evolutionary
447 demographic responses to climate change: Taking theory out to the field. *Functional*
448 *Ecology*, *27*(4), 967–979. https://doi.org/10.1111/j.1365-2435.2012.02043.x
449 Clusella-Trullas, S., Blackburn, T. M., & Chown, S. L. (2011). Climatic Predictors of
450 Temperature Performance Curve Parameters in Ectotherms Imply Complex Responses to
451 Climate Change. *The American Naturalist*, *177*(6), 738–751.
452 https://doi.org/10.1086/660021
453 Condon, C., Acharya, A., Adrian, G. J., Hurliman, A. M., Malekooti, D., Nguyen, P., Zelic, M.
454 H., & Angilletta Jr, M. J. (2015). Indirect selection of thermal tolerance during
455 experimental evolution of Drosophila melanogaster. *Ecology and Evolution*, *5*(9), 1873–
456 1880. https://doi.org/10.1002/ece3.1472
457 Cox, R. M., & Calsbeek, R. (2014). Survival of the fattest? Indices of body condition do not
458 predict viability in the brown anole (Anolis sagrei). *Functional Ecology*, *29*(3), 404–413.
459 https://doi.org/10.1111/1365-2435.12346
460 Deutsch, C. A., Tewksbury, J. J., Huey, R. B., Sheldon, K. S., Ghalambor, C. K., Haak, D. C., &
461 Martin, P. R. (2008). Impacts of climate warming on terrestrial ectotherms across
462 latitude. *Proceedings of the National Academy of Sciences*, *105*(18), 6668–6672.
463 https://doi.org/10.1073/pnas.0709472105
464 Elmhagen, B., Kindberg, J., Hellström, P., & Angerbjörn, A. (2015). A boreal invasion in
465 response to climate change? Range shifts and community effects in the borderland

between forest and tundra. *AMBIO*, *44*(1), 39–50. https://doi.org/10.1007/s13280-014-0606-8

Fey, S. B., Vasseur, D. A., Alujević, K., Kroeker, K. J., Logan, M. L., O'Connor, M. I., Rudolf, V. H. W., DeLong, J. P., Peacor, S., Selden, R. L., Sih, A., & Clusella-Trullas, S. (2019). Opportunities for behavioral rescue under rapid environmental change. *Global Change Biology*, *25*(9), 3110–3120. https://doi.org/10.1111/gcb.14712

Fisher, R. A. (1958). *The genetical theory of natural selection*. Рипол Классик.

Fox, R. J., Donelson, J. M., Schunter, C., Ravasi, T., & Gaitán-Espitia, J. D. (2019). Beyond buying time: The role of plasticity in phenotypic adaptation to rapid environmental change. *Philosophical Transactions of the Royal Society B: Biological Sciences*, *374*(1768), 20180174. https://doi.org/10.1098/rstb.2018.0174

Frankham, R. (1996). Relationship of Genetic Variation to Population Size in Wildlife. *Conservation Biology*, *10*(6), 1500–1508. https://doi.org/10.1046/j.1523-1739.1996.10061500.x

Gilchrist, G. W. (1995). Specialists and Generalists in Changing Environments. I. Fitness Landscapes of Thermal Sensitivity. *The American Naturalist*, *146*(2), 252–270. https://doi.org/10.1086/285797

Gilchrist, G. W. (1996). A Quantitative Genetic Analysis of Thermal Sensitivity in the Locomotor Performance Curve of Aphidius Ervi. *Evolution*, *50*(4), 1560–1572. https://doi.org/10.1111/j.1558-5646.1996.tb03928.x

Gilchrist, G. W., Huey, R. B., & Partridge, L. (1997). Thermal Sensitivity of Drosophila melanogaster: Evolutionary Responses of Adults and Eggs to Laboratory Natural

Selection at Different Temperatures. *Physiological Zoology*, *70*(4), 403–414. https://doi.org/10.1086/515853

Grant, P. R., & Grant, B. R. (2002). Unpredictable Evolution in a 30-Year Study of Darwin's Finches. *Science*. https://doi.org/10.1126/science.1070315

Hairston, N. G., Ellner, S. P., Geber, M. A., Yoshida, T., & Fox, J. A. (2005). Rapid evolution and the convergence of ecological and evolutionary time. *Ecology Letters*, *8*(10), 1114–1127. https://doi.org/10.1111/j.1461-0248.2005.00812.x

Hochachka, P. W., & Somero, G. N. (2002). *Biochemical Adaptation: Mechanism and Process in Physiological Evolution*. Oxford University Press.

Hoffmann, A. A., & Sgrò, C. M. (2011). Climate change and evolutionary adaptation. *Nature*, *470*(7335), 479–485. https://doi.org/10.1038/nature09670

Huey, R. B., Hertz, P. E., & Sinervo, B. (2003). Behavioral Drive versus Behavioral Inertia in Evolution: A Null Model Approach. *The American Naturalist*, *161*(3), 357–366. https://doi.org/10.1086/346135

Huey, R. B., & Stevenson, R. D. (1979). Integrating Thermal Physiology and Ecology of Ectotherms: A Discussion of Approaches. *American Zoologist*, *19*(1), 357–366. https://doi.org/10.1093/icb/19.1.357

Izem, R., & Kingsolver, J. G. (2005). Variation in Continuous Reaction Norms: Quantifying Directions of Biological Interest. *The American Naturalist*, *166*(2), 277–289. https://doi.org/10.1086/431314

Kearney, M., Shine, R., & Porter, W. P. (2009). The potential for behavioral thermoregulation to buffer "cold-blooded" animals against climate warming. *Proceedings of the National Academy of Sciences*, *106*(10), 3835–3840. https://doi.org/10.1073/pnas.0808913106

Kingsolver, J. G., & Diamond, S. E. (2015). Phenotypic Selection in Natural Populations: What Limits Directional Selection? *The American Naturalist*. https://doi.org/10.1086/658341

Kingsolver, J. G., Heckman, N., Zhang, J., Carter, P. A., Knies, J. L., Stinchcombe, J. R., & Meyer, K. (2015). Genetic Variation, Simplicity, and Evolutionary Constraints for Function-Valued Traits. *The American Naturalist*, *185*(6), E166–E181. https://doi.org/10.1086/681083

Kingsolver, J. G., Ragland, G. J., & Shlichta, J. G. (2004). Quantitative Genetics of Continuous Reaction Norms: Thermal Sensitivity of Caterpillar Growth Rates. *Evolution*, *58*(7), 1521–1529. https://doi.org/10.1111/j.0014-3820.2004.tb01732.x

Knies, J. L., Izem, R., Supler, K. L., Kingsolver, J. G., & Burch, C. L. (2006). The Genetic Basis of Thermal Reaction Norm Evolution in Lab and Natural Phage Populations. *PLOS Biology*, *4*(7), e201. https://doi.org/10.1371/journal.pbio.0040201

Knies, J. L., Kingsolver, J. G., & Burch, C. L. (2009). Hotter Is Better and Broader: Thermal Sensitivity of Fitness in a Population of Bacteriophages. *The American Naturalist*, *173*(4), 419–430. https://doi.org/10.1086/597224

Lande, R. (1993). Risks of Population Extinction from Demographic and Environmental Stochasticity and Random Catastrophes. *The American Naturalist*, *142*(6), 911–927. https://doi.org/10.1086/285580

Latimer, C. a. L., Wilson, R. S., & Chenoweth, S. F. (2011). Quantitative genetic variation for thermal performance curves within and among natural populations of Drosophila serrata. *Journal of Evolutionary Biology*, *24*(5), 965–975. https://doi.org/10.1111/j.1420-9101.2011.02227.x

Logan, M. L., & Cox, C. L. (2020). Genetic Constraints, Transcriptome Plasticity, and the Evolutionary Response to Climate Change. *Frontiers in Genetics*, *0*. https://doi.org/10.3389/fgene.2020.538226

Logan, M. L., Cox, R. M., & Calsbeek, R. (2014). Natural selection on thermal performance in a novel thermal environment. *Proceedings of the National Academy of Sciences*, *111*(39), 14165–14169. https://doi.org/10.1073/pnas.1404885111

Logan, M. L., Curlis, J. D., Gilbert, A. L., Miles, D. B., Chung, A. K., McGlothlin, J. W., & Cox, R. M. (2018). Thermal physiology and thermoregulatory behaviour exhibit low heritability despite genetic divergence between lizard populations. *Proceedings of the Royal Society B: Biological Sciences*. https://doi.org/10.1098/rspb.2018.0697

Logan, M. L., Minnaar, I. A., Keegan, K. M., & Clusella-Trullas, S. (2020). The evolutionary potential of an insect invader under climate change*. *Evolution*, *74*(1), 132–144. https://doi.org/10.1111/evo.13862

Logan, M. L., Neel, L. K., Nicholson, D. J., Stokes, A. J., Miller, C. L., Chung, A. K., Curlis, J. D., Keegan, K. M., Rosso, A. A., Maayan, I., Folfas, E., Williams, C. E., Casement, B., Gallegos Koyner, M. A., Padilla Perez, D. J., Falvey, C. H., Alexander, S. M., Charles, K. L., Graham, Z. A., … Cox, C. L. (2021). Sex-specific microhabitat use is associated with sex-biased thermal physiology in Anolis lizards. *Journal of Experimental Biology*, *224*(2). https://doi.org/10.1242/jeb.235697

Logan, M. L., van Berkel, J., & Clusella-Trullas, S. (2019). The Bogert Effect and environmental heterogeneity. *Oecologia*, *191*(4), 817–827. https://doi.org/10.1007/s00442-019-04541-7

Losos, J. B. (2011). *Lizards in an Evolutionary Tree: Ecology and Adaptive Radiation of Anoles*. Univ of California Press.

Martins, F., Kruuk, L., Llewelyn, J., Moritz, C., & Phillips, B. (2019). Heritability of climate-relevant traits in a rainforest skink. *Heredity*, *122*(1), 41–52. https://doi.org/10.1038/s41437-018-0085-y

Muñoz, M. M. (2022). The Bogert effect, a factor in evolution. *Evolution*, *76*(S1), 49–66. https://doi.org/10.1111/evo.14388

Neel, L. K., Logan, M. L., Nicholson, D. J., Miller, C., Chung, A. K., Maayan, I., Degon, Z., DuBois, M., Curlis, J. D., Taylor, Q., Keegan, K. M., McMillan, W. O., Losos, J. B., & Cox, C. L. (2021). Habitat structure mediates vulnerability to climate change through its effects on thermoregulatory behavior. *Biotropica*, *53*(4), 1121–1133. https://doi.org/10.1111/btp.12951

O'Grady, J. J., Reed, D. H., Brook, B. W., & Frankham, R. (2004). What are the best correlates of predicted extinction risk? *Biological Conservation*, *118*(4), 513–520. https://doi.org/10.1016/j.biocon.2003.10.002

Padmavathi, C., Katti, G., Sailaja, V., Padmakumari, A. P., Jhansilakshmi, V., Prabhakar, M., & Prasad, Y. G. (2013). Temperature Thresholds and Thermal Requirements for the Development of the Rice Leaf Folder, Cnaphalocrocis medinalis. *Journal of Insect Science*, *13*, 96. https://doi.org/10.1673/031.013.9601

Phillips, B. L., Llewelyn, J., Hatcher, A., Macdonald, S., & Moritz, C. (2014). Do evolutionary constraints on thermal performance manifest at different organizational scales? *Journal of Evolutionary Biology*, *27*(12), 2687–2694. https://doi.org/10.1111/jeb.12526

Richter-Boix, A., Katzenberger, M., Duarte, H., Quintela, M., Tejedo, M., & Laurila, A. (2015). Local divergence of thermal reaction norms among amphibian populations is affected by

pond temperature variation. *Evolution*, *69*(8), 2210–2226. https://doi.org/10.1111/evo.12711

Roff, D. A., & Fairbairn, D. J. (2012). A Test of the Hypothesis That Correlational Selection Generates Genetic Correlations. *Evolution*, *66*(9), 2953–2960. https://doi.org/10.1111/j.1558-5646.2012.01656.x

Schlötterer, C., Kofler, R., Versace, E., Tobler, R., & Franssen, S. U. (2015). Combining experimental evolution with next-generation sequencing: A powerful tool to study adaptation from standing genetic variation. *Heredity*, *114*(5), 431–440. https://doi.org/10.1038/hdy.2014.86

Schou, M. F., Engelbrecht, A., Brand, Z., Svensson, E. I., Cloete, S., & Cornwallis, C. K. (2022). Evolutionary trade-offs between heat and cold tolerance limit responses to fluctuating climates. *Science Advances*. https://doi.org/10.1126/sciadv.abn9580

Sears, M. W., & Angilletta, M. J. (2015). Costs and Benefits of Thermoregulation Revisited: Both the Heterogeneity and Spatial Structure of Temperature Drive Energetic Costs. *The American Naturalist*, *185*(4), E94–E102. https://doi.org/10.1086/680008

Sears, M. W., Angilletta, M. J., Schuler, M. S., Borchert, J., Dilliplane, K. F., Stegman, M., Rusch, T. W., & Mitchell, W. A. (2016). Configuration of the thermal landscape determines thermoregulatory performance of ectotherms. *Proceedings of the National Academy of Sciences*, *113*(38), 10595–10600. https://doi.org/10.1073/pnas.1604824113

Sinervo, B., Méndez-de-la-Cruz, F., Miles, D. B., Heulin, B., Bastiaans, E., Cruz, M. V.-S., Lara-Resendiz, R., Martínez-Méndez, N., Calderón-Espinosa, M. L., Meza-Lázaro, R. N., Gadsden, H., Avila, L. J., Morando, M., Riva, I. J. D. la, Sepulveda, P. V., Rocha, C. F. D., Ibargüengoytía, N., Puntriano, C. A., Massot, M., … Jack W. Sites, J. (2010). Erosion

of Lizard Diversity by Climate Change and Altered Thermal Niches. *Science*. https://doi.org/10.1126/science.1184695

Teotónio, H., Chelo, I. M., Bradić, M., Rose, M. R., & Long, A. D. (2009). Experimental evolution reveals natural selection on standing genetic variation. *Nature Genetics*, *41*(2), 251–257. https://doi.org/10.1038/ng.289

van Berkum, F. H. (1986). Evolutionary Patterns of the Thermal Sensitivity of Sprint Speed in Anolis Lizards. *Evolution*, *40*(3), 594–604. https://doi.org/10.1111/j.1558-5646.1986.tb00510.x

Vasseur, D. A., DeLong, J. P., Gilbert, B., Greig, H. S., Harley, C. D. G., McCann, K. S., Savage, V., Tunney, T. D., & O'Connor, M. I. (2014). Increased temperature variation poses a greater risk to species than climate warming. *Proceedings of the Royal Society B: Biological Sciences*. https://doi.org/10.1098/rspb.2013.2612

Figures

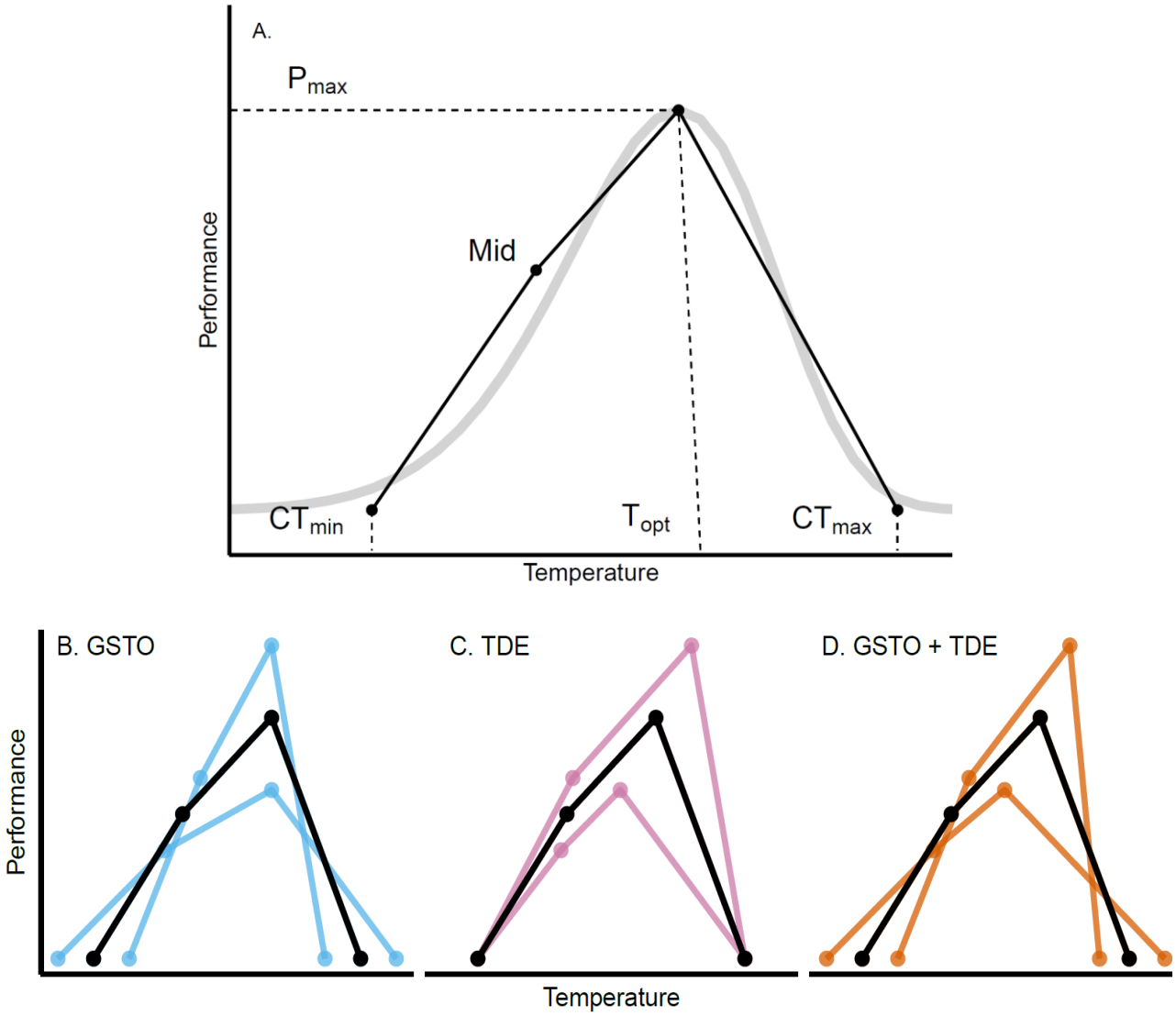

Figure 1. The general structure of thermal performance curves (TPCs) and genetic correlations in our simulations. (a) We used a minimum convex polygon approach (black polygon) to approximate a traditional non-linear TPC function (gray curve). (b-d) Phenotypic variability in TPC shapes under the generalist-specialist trade-off (GSTO, b), the thermodynamic effect (TDE, c) and both the GSTO and the TDE simultaneously (GSTO + TDE, d). For panels b-d, black TPC polygons indicate population averages while colored polygons indicate extreme phenotypes.

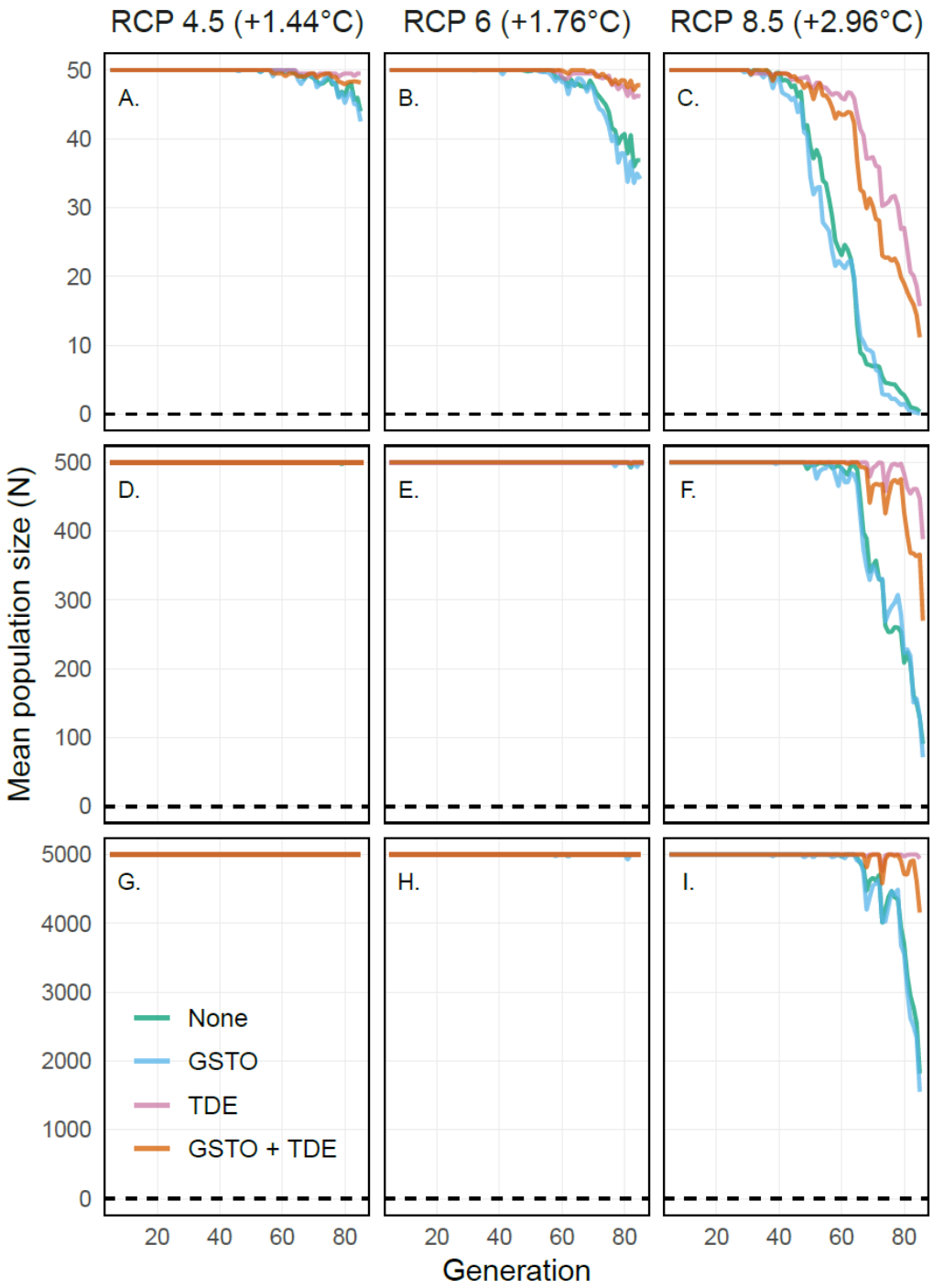

Figure 2. Changes in average population size over 80 generations (80 years) of environmental change. Populations were exposed to three different climate change scenarios (columns) and starting population sizes (rows). For each pairwise combination of starting population size and climate change scenario, we modeled changes in population size for populations whose TPC shapes were unconstrained by genetic correlations (None, green lines), or constrained by a generalist-specialist trade-off (GSTO, blue lines), a thermodynamic effect (TDE, purple lines), or both a generalist-specialist trade-off and a thermodynamic effect (GSTO + TDE, orange lines). In all cases, lines indicate the mean population size (N) for 100 simulation replicates.

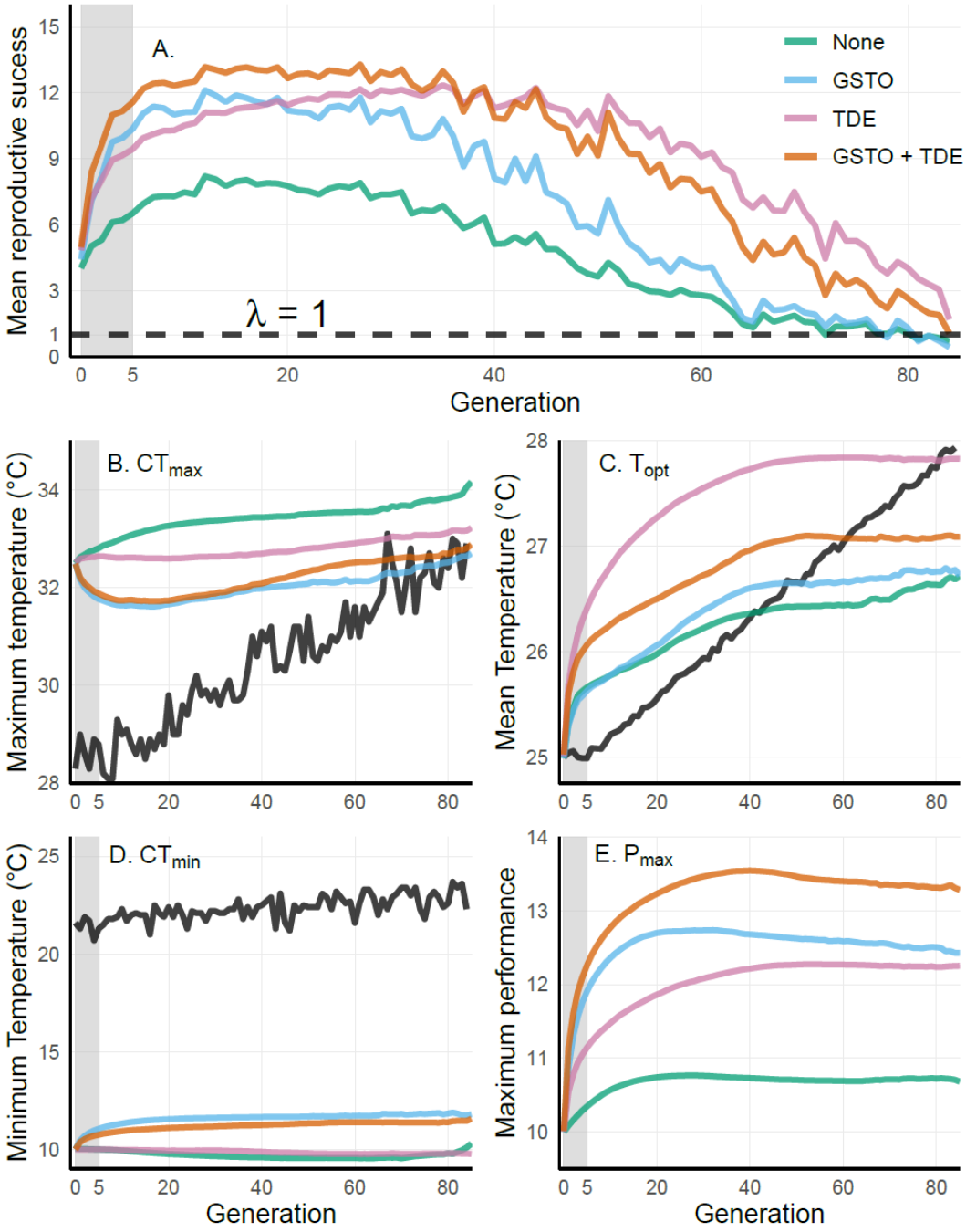

644
645
646 **Figure 3.** Mean reproductive success (A) and evolutionary change in thermal performance traits
647 (B-E) with respect to changes in the thermal environment across all N_0 = 500 populations
648 exposed to the RCP 8.5 climate change scenario. For all panels, colored lines indicate the genetic
649 correlation populations were subjected to and correspond to the mean across 100 simulation
650 replicates. "None" indicates unconstrained populations (green), "GSTO" indicates populations
651 subjected to the generalist-specialist trade-off (blue), "TDE" indicates populations subject to the
652 thermodynamic effect (purple) and "GSTO + TDE" indicates populations subjected to both the
653 generalist-specialist trade-off and thermodynamic effect (orange). The shaded areas indicate the
654 burn-in period (generations 0-5) where no environmental change occurred. For panel A, the

black dashed line indicates a mean reproductive success of 1 ($\lambda = 1$), above which a population would grow and below which it would decline. For panels B-D, black lines indicate the maximum (B), mean (C) and minimum (D) environmental temperatures experienced each generation while colored lines indicate changes in CT_{max} (B), T_{opt} (C), CT_{min} (D), and P_{max} (E).

Supplementary Materials

1. Methodological Details

Generating starting populations

Each starting population was composed of a set of unique TPCs. To construct these TPCs, we used four baseline 'thermal performance traits' which are commonly used to describe TPCs in empirical studies (and thus their evolution is easily interpretable; Logan et al., 2014; Logan & Cox, 2020). These traits were the thermal optimum (T_{opt}), the critical thermal limits (CT_{min} & CT_{max}), maximum performance (P_{max}), and an intermediate temperature point (which we term "Mid") between CT_{min} and T_{opt} to allow for the stereotypical left skewness of TPCs (Angilletta, 2006). We chose a set of base values for each of these traits (T_{opt} = 25° C, CT_{min} = 10° C, CT_{max} = 35° C, P_{max} = 10) with "Mid" being at a temperature value of 19°C (halfway between the base values of CT_{min} and T_{opt}) and a performance value of 5 (the P_{max} base value divided by two). The specific base values are arbitrary and not crucial for interpreting the role of genetic correlations (see below), although we chose these values because they are similar to what has been measured in real populations of mid-latitude ectotherms (e.g. Padmavathi et al., 2013). To generate among-individual variation in TPC shapes within each starting population, we randomized the base values using the following formula:

$$Randomized\ Trait = Base\ Trait + QG \quad (1)$$

$$Q \sim \mathrm{N}(0,1) \quad (2)$$

Whereby a base value would be modified by adding a quantity (Q) sampled from a normal distribution of mean = 0 and standard deviation = 1, and then multiplied by a genetic variance-

covariance matrix (*G*) to obtain the randomized value. We used a different *G*-matrix to generate populations according to each genetic correlation scenario. For populations governed by only a GSTO, we used the following *G*:

$$G_{GSTO} = \begin{array}{c} \begin{matrix} CT_{min} & Mid & T_{opt} & CT_{max} & P_{max} \end{matrix} \\ \begin{bmatrix} 1 & 0 & 0 & 0 & 0.75 \\ 0 & 1 & 0 & 0 & 0.75 \\ 0 & 0 & 1 & 0 & 0 \\ 0 & 0 & 0 & 1 & -0.75 \\ 0.75 & 0.75 & 0 & -0.75 & 1 \end{bmatrix} \begin{matrix} CT_{min} \\ Mid \\ T_{opt} \\ CT_{max} \\ P_{max} \end{matrix} \end{array} \quad (3)$$

This matrix included a positive correlation between P_{max} and both CT_{min} and *Mid*, and a negative correlation between P_{max} and CT_{max}, because a GSTO should result in reduced maximal performance capacity when performance increases at or near the tolerance limits. Here and below, we used a genetic correlation strength of 0.75 (or -0.75) such that correlations were strong but not overwhelmingly so. For populations governed by only the TDE, we used the following *G*:

$$G_{TDE} = \begin{array}{c} \begin{matrix} CT_{min} & Mid & T_{opt} & CT_{max} & P_{max} \end{matrix} \\ \begin{bmatrix} 1 & 0 & 0 & 0 & 0 \\ 0 & 1 & 0 & 0 & 0 \\ 0 & 0 & 1 & 0 & 0.75 \\ 0 & 0 & 0 & 1 & 0 \\ 0 & 0 & 0.75 & 0 & 1 \end{bmatrix} \begin{matrix} CT_{min} \\ Mid \\ T_{opt} \\ CT_{max} \\ P_{max} \end{matrix} \end{array} \quad (4)$$

This matrix included a positive correlation between T_{opt} and P_{max}, but no other correlations, because this is the sole relationship among thermal performance traits that defines the TDE. For populations governed by both a GSTO and a TDE, we used the following *G*:

$$G_{GSTO+TDE} = \begin{array}{c} \begin{matrix} CT_{min} & Mid & T_{opt} & CT_{max} & P_{max} \end{matrix} \\ \left[\begin{matrix} 1 & 0 & 0 & 0 & 0.75 \\ 0 & 1 & 0 & 0 & 0.75 \\ 0 & 0 & 1 & 0 & 0.75 \\ 0 & 0 & 0 & 1 & -0.75 \\ 0.75 & 0.75 & 0.75 & -0.75 & 1 \end{matrix}\right] \end{array} \begin{matrix} CT_{min} \\ Mid \\ T_{opt} \\ CT_{max} \\ P_{max} \end{matrix} \quad (5)$$

This matrix included all pairwise genetic correlations that are expected when both a GSTO and a TDE are present in the same population. Finally, for populations whose TPC shapes were not constrained by genetic correlations, *G* was defined as a 5 × 5 identity matrix with all correlations among traits set to zero.

After obtaining the final set of trait values defining an individual's TPC, we removed or corrected any values that would result in TPCs with impossible shapes. For example, we corrected instances in which the trait randomization or the multiplication by *G* had resulted in individuals with $CT_{min} > T_{opt}$ or $CT_{max} < T_{opt}$. After removal of these individuals, the remaining values were used as the basis to generate a unique TPC for each individual. We used a simple minimum convex polygon algorithm to construct TPCs from trait values (Angilletta, 2009; van Berkum, 1986). We built TPCs by linearly connecting adjacent trait values to form a polygon that approximated the shape of the curve (Figure 1A). As opposed to curve-fitting (an alternative approach used in empirical studies, e.g. Angilletta, 2006), this procedure ensured that the genetic correlations specified in *G* would be perfectly represented in the trait distribution of each starting

751 population because there were no parameters with pre-existing correlation structures (as would
752 often be the case when curve fitting; Figure S2). For each combination of genetic correlation
753 scenario and starting population size (4 x 3), we generated 10 unique populations (based on the
754 same *G*) to avoid the possibility of drawing general conclusions from a single anomalous starting
755 trait distribution.
756
757 **Simulating thermal environments**
758 For all simulations, we set the initial environmental conditions to a mean daily environmental
759 temperature (T_m) of 25 °C and a standard deviation (T_{sd}) of 1 °C. Thus, all populations started
760 out in a relatively stable thermal environment that closely matched the characteristics of their
761 TPCs (i.e., they were locally adapted). We simulated climate change following the RCP 4.5
762 (ΔT_m = 1.44 °C), RCP 6 (ΔT_m = 1.76 °C), and RCP 8.5 (ΔT_m = 2.96 °C) IPCC scenarios through
763 the year 2100. For all IPCC scenarios, we assumed a 15% increase in T_{sd} for every 1°C increase
764 in T_m following Bathinay et al. (2018). We also included a set of control simulations in which
765 thermal conditions did not change (ΔT_m = 0 °C, ΔT_{sd} = 0 °C). In addition to these three IPCC
766 scenarios and the control, we generated four more temperature change scenarios to tease apart
767 the effects of specific environmental and climate change features on population dynamics and
768 TPC evolution. For these, we used the RCP 8.5 scenario but kept either ΔT_m or ΔT_{sd} at zero
769 while allowing the other to change. We included additional RCP 8.5 simulations (again with
770 control simulations) but with double the initial T_{sd} (2°C) to explore the effects of a more variable
771 starting thermal environment on subsequent population dynamics and evolution.
772 To generate the specific thermal environments that a given population was exposed to
773 each generation, we first defined a sequence of 80 T_m and T_{sd} values (one for each year or

774 generation with a 5-year burn-in). These values increased linearly following the particular
775 climate change scenario being modeled. Within each generation, these base values were then
776 used to generate a normal distribution from which we sampled 150 daily temperatures. We chose
777 150 days to represent the breeding season of our hypothetical ectotherm, as this is similar to the
778 length of this period in some real species (e.g. Cox & Calsbeek, 2014), although the specific
779 length of the breeding season is unlikely to impact the results of simulations. For all simulations,
780 we introduced a "burn-in" period of five generations during which we did not allow the thermal
781 environment to change such that populations could further adapt to local conditions. For each
782 climate change scenario, we generated 10 unique sequences of temperature change (but from the
783 same starting environmental temperature distribution in each generation) to ensure that our
784 results were robust to anomalous years arising from the random sampling of the temperature
785 distribution in any given generation.
786
787 **Modeling survival and reproduction**
788 In our simulations, changes in population size ultimately arose from variation in the survival and
789 reproductive success of individuals, much as it would in real populations. For each day in a given
790 simulation, the performance of each individual was calculated by combining information about
791 the daily environmental temperature with individuals' TPCs. Specifically, we calculated an
792 individual's performance from its TPC and then used this performance value to generate a daily
793 survival probability according to the following expression:
794

$$P(S)_i = (1 + e^{-(\alpha + \beta p_i)})^{-1} \quad (6)$$

795

Where, for a given day (i) the probability of surviving $(P(S)_i)$ is related to the individual's performance (p_i) through a logistic function. In all cases, the values of the parameters α and β were set to -5 and 1 respectively such that $P(S)_i = 0.5$ when $p_i = 5$, with the value of 5 being a performance exactly half of the base value of P_{max}. We then used each individual's $P(S)$ on a particular day to calculate its actual survival (S) such that:

$$S_i \sim Bernoulli(P(S)_i) \quad (7)$$

This approach adds a stochastic component to survival which more closely mimics the dynamics of real populations and produces a binary outcome of either death (0) or survival (1) for every individual on every day of the simulation. After an individual reached a value of $S = 0$ for a given day, it would be considered dead for all remaining days within that generation. We then calculated reproductive success (R_g) of each individual as:

$$R_g = \left\lfloor \frac{1}{10} \sum_{i}^{150} S_i \right\rfloor \quad (8)$$

Whereby reproductive success within a generation (R_g) was an integer corresponding to 10% of the rounded-down sum of all survived days within a generation. Since the number of days within a generation was set at 150, the maximum possible reproductive output for any individual through an entire generation was 15, and an individual had to survive at least 10 days in order to produce one offspring. This simulation structure mimics the often empirically measured "viability selection", whereby longer survival over the breeding season is assumed to lead to

816 greater reproductive success and follows the breeding biology of some well-known vertebrate
817 groups such as *Anolis* lizards (Losos, 2011). Because individuals are represented solely by their
818 TPCs, offspring produced by an individual were assigned the exact same TPC as the parent (i.e.,
819 asexual cloning with a heritability of 1). Lastly, if the number of newly generated individuals
820 exceeded the initial population size (carrying capacity), a random sample of offspring that
821 equaled the carrying capacity was drawn to form the population for the next generation.
822 We ran unique simulations for every combination of genetic correlation and thermal
823 environment. For example, when exposing GSTO-constrained populations to the RCP 4.5
824 scenario, we ran a simulation exposing each of the 10 population replicates (based on same base
825 values but differing because of randomization around those values) to each of the 10 thermal
826 environment replicates (based on the same change in mean and standard deviation but differing
827 because of random sampling of the temperature distribution within each generation) for a total of
828 100 simulations. For each combination of genetic correlation and thermal environment,
829 population sizes and TPC characteristics were recorded as the average of the 100 simulations in
830 each generation. We did this for all 64 combinations presented in Tables S1 and S2 which totaled
831 6400 unique individual-based simulations.
832
833
834
835
836
837
838
839
840
841
842
843
844

2. Supplementary Figures:

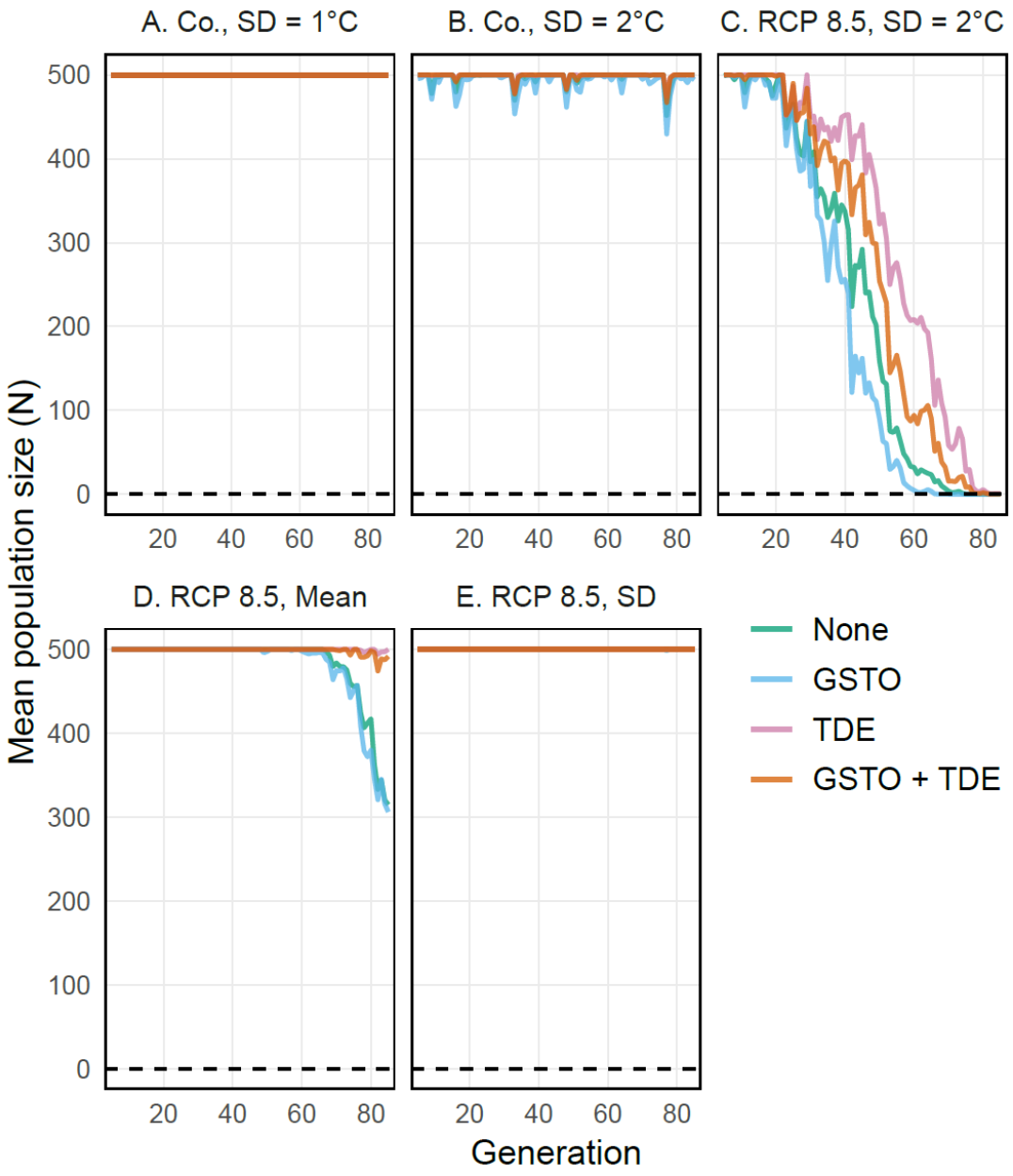

Figure S1. Changes in population size across different simulated conditions. Each panel indicates the climate change scenario to which populations were exposed to; a control (Co.) with no environmental change (with initial standard deviation (SD) in temperature of 1°C) (a), a control with a more thermally variable environment (Initial SD = 2°C) (b), the RCP 8.5 climate change scenario on an initially more variable thermal environment (+ 2.96°C in mean temperature & Initial SD = 2°C) (c) and the RCP 8.5 scenario with only changes in mean daily temperature (e) or standard deviation in temperature (f) with Initial SD = 1°C. Line color indicates the genetic correlation to which populations were subject to. In all cases, N_0 & K = 500 and lines indicate the mean population size (N) for 100 simulation replicates.

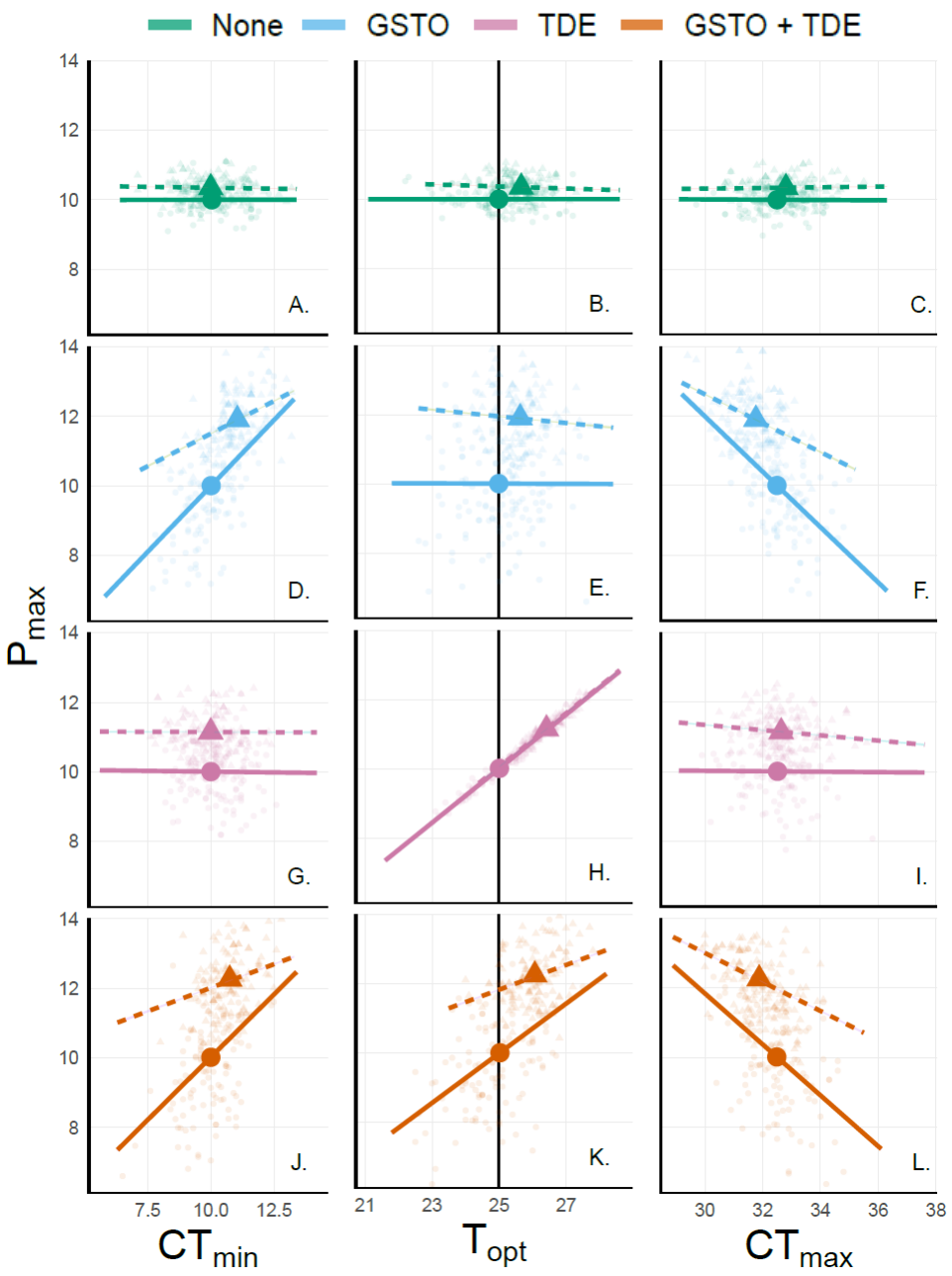

Figure S2. Relationship between P_{max} and T_{opt} (left column) and P_{max} and CT_{max} (right column, as a representative of TPC breath) in simulations where N_0 & K = 500 populations were exposed to the RCP 8.5 climate change scenario at the start (generation 0, solid line & circles) and the end of the acclimation period (generation 5, dashed line & triangles). Rows and color indicate the genetic correlation each population was subjected to. The solid point indicates the mean phenotype of the population, and the line indicates the distribution and range of phenotypes across the entire population. Light background points show a representative sample of phenotypic variability.

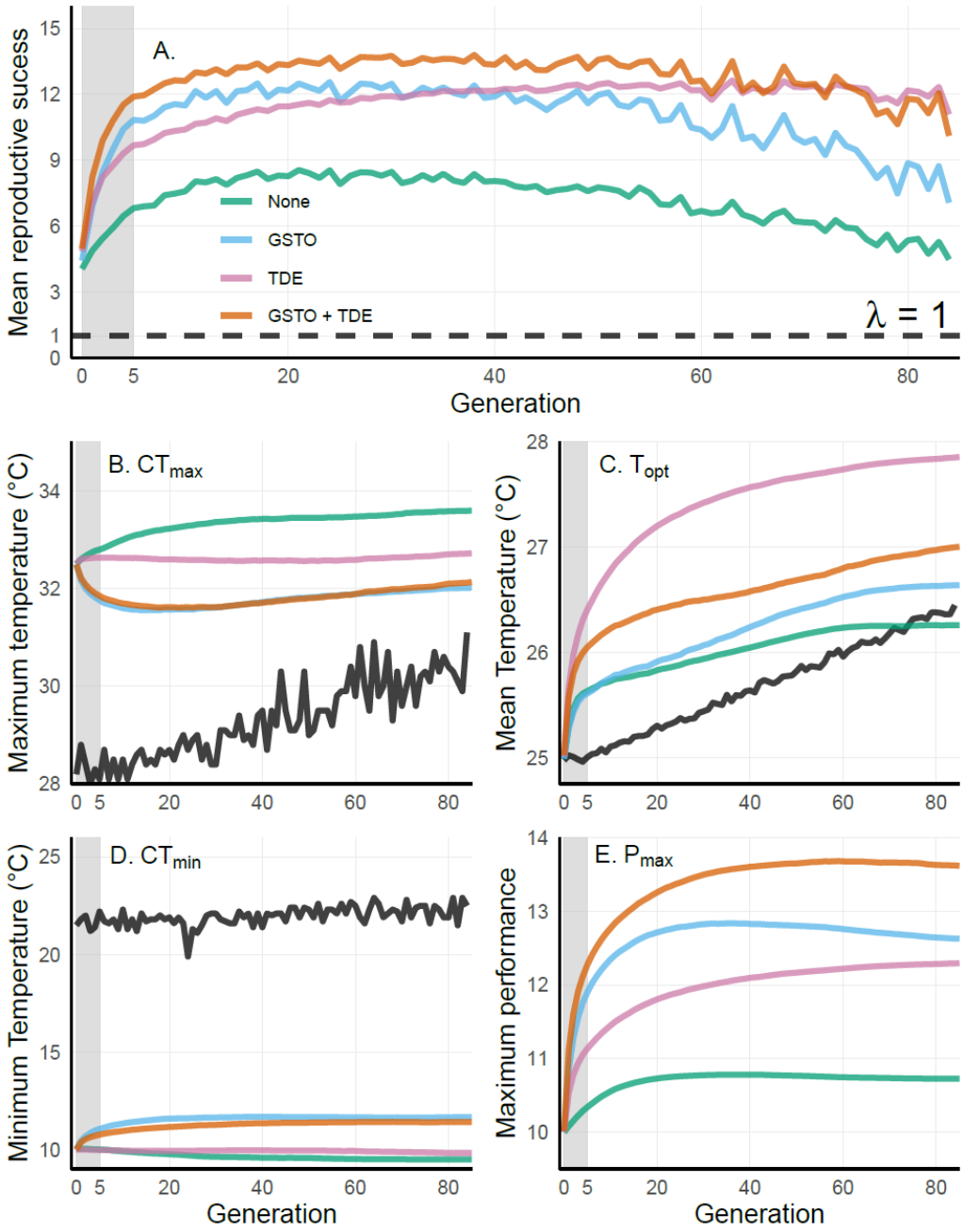

Figure S3. Mean reproductive success (A) and evolutionary change in thermal performance traits (B-E) with respect to changes in the thermal environment across all N_0 = 500 populations exposed to the RCP 4.5 climate change scenario. For all panels, colored lines indicate the genetic correlation populations were subjected to and correspond to the mean across 100 simulation replicates. "None" indicates unconstrained populations (green), "GSTO" indicates populations subjected to the generalist-specialist trade-off (blue), "TDE" indicates populations subject to the thermodynamic effect (purple) and "GSTO + TDE" indicates populations subjected to both the generalist-specialist trade-off and thermodynamic effect (orange). The shaded areas indicate the burn-in period (generations 0-5) where no environmental change occurred. For panel A, the

black dashed line indicates a mean reproductive success of 1 ($\lambda = 1$), above which a population would grow and below which it would decline. For panels B-D, black lines indicate the maximum (B), mean (C) and minimum (D) environmental temperatures experienced each generation while colored lines indicate changes in CT_{max} (B), T_{opt} (C), CT_{min} (D), and P_{max} (E).

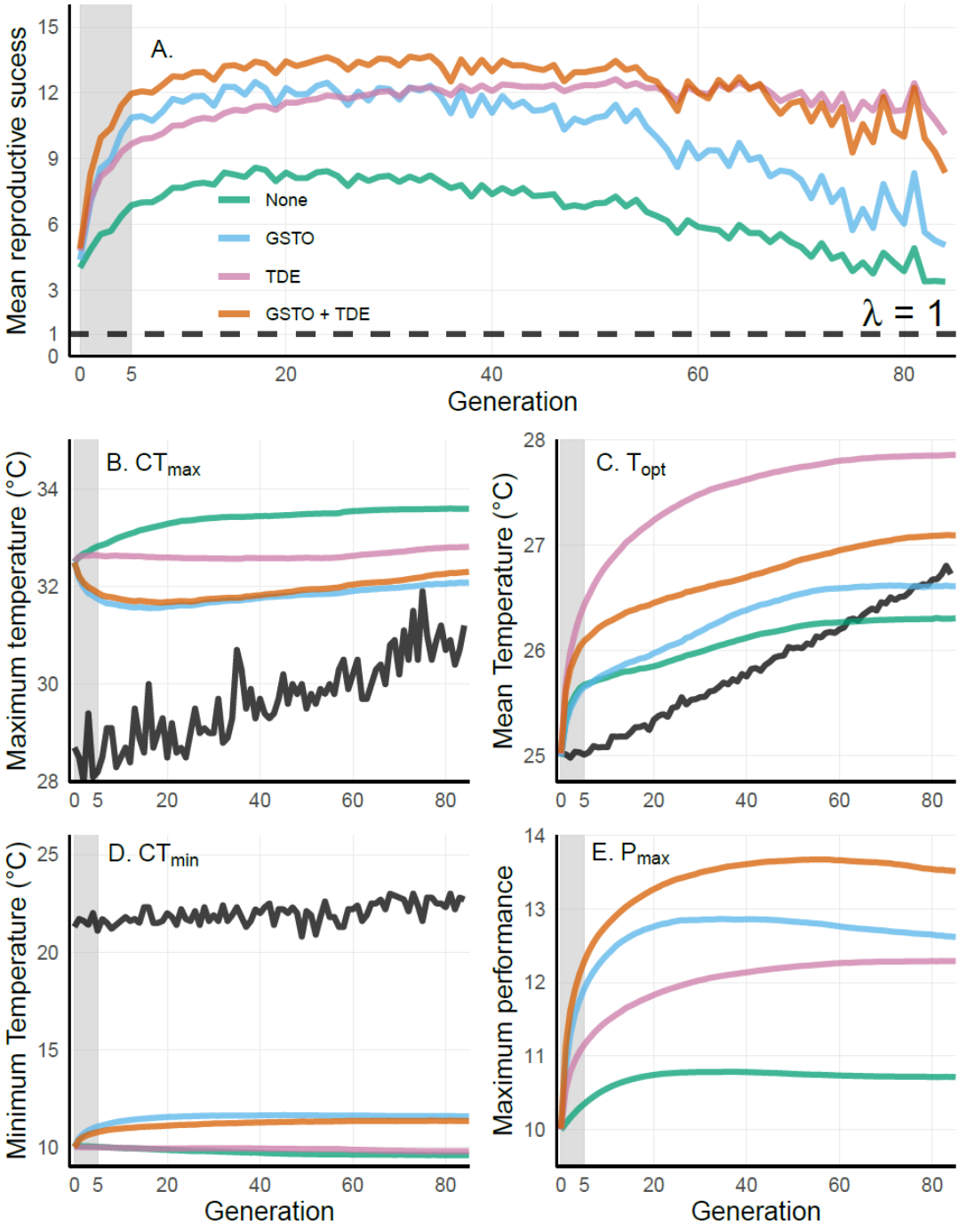

Figure S4. Mean reproductive success (A) and evolutionary change in thermal performance traits (B-E) with respect to changes in the thermal environment across all N_0 = 500 populations exposed to the RCP 6 climate change scenario. For all panels, colored lines indicate the genetic correlation populations were subjected to and correspond to the mean across 100 simulation replicates. "None" indicates unconstrained populations (green), "GSTO" indicates populations subjected to the generalist-specialist trade-off (blue), "TDE" indicates populations subject to the thermodynamic effect (purple) and "GSTO + TDE" indicates populations subjected to both the

generalist-specialist trade-off and thermodynamic effect (orange). The shaded areas indicate the burn-in period (generations 0-5) where no environmental change occurred. For panel A, the black dashed line indicates a mean reproductive success of 1 ($\lambda = 1$), above which a population would grow and below which it would decline. For panels B-D, black lines indicate the maximum (B), mean (C) and minimum (D) environmental temperatures experienced each generation while colored lines indicate changes in CT_{max} (B), T_{opt} (C), CT_{min} (D), and P_{max} (E).

3. Supplementary Tables

Table S1. Population sizes and percentage of population decline across different simulated conditions based on IPCC climate change models.

Genetic Correlation	N_0 & K	Climate Change Scenario: Control	RCP 4.5	RCP 6	RCP 8.5	$\overline{RCP}$	$\overline{RCP}$ per Genetic Correlation
None	**50**	50 (0%)	44.04 (11.92%)	36.91 (26.18%)	0.35 (99.3%)	27.1 (45.8%)	32.56%
	500	500 (0%)	500 (0%)	497.92 (0.4%)	41.86 (91.63%)	346.59 (30.68%)	
	5000	5000 (0%)	5000 (0%)	5000 (0%)	1818.51 (63.62%)	3939.5 (21.21%)	
GSTO	**50**	50 (0%)	42.55 (14.9%)	34.20 (31.6%)	0.07 (99.86%)	25.61 (48.79%)	34.54%
	500	500 (0%)	500 (0%)	499.53 (0.09%)	22.90 (95.42%)	340.81 (31.84%)	
	5000	5000 (0%)	5000 (0%)	5000 (0%)	1554.22 (68.92%)	3851.41 (22.97%)	
TDE	**50**	50 (0%)	49.50 (1%)	46.18 (7.64%)	15.71 (68.58%)	37.13 (25.74%)	11.36%
	500	500 (0%)	500 (0%)	500 (0%)	380.59 (23.88%)	460.2 (7.96%)	
	5000	5000 (0%)	5000 (0%)	5000 (0%)	4943.58 (1.1%)	4981.2 (0.38%)	
GSTO + TDE	**50**	50 (0%)	48.17 (3.66%)	47.78 (4.44%)	11.17 (77.66%)	35.71 (28.59%)	17.35%
	500	500 (0%)	500 (0%)	500 (0%)	232.12 (53.57%)	410.71 (17.86%)	
	5000	5000 (0%)	5000 (0%)	5000 (0%)	4159.54 (16.81%)	4719.85 (5.6%)	
		0%	2.62%	5.86%	63.376%	23.85%	

Table S2. Population sizes and percentage of population decline across experimentally simulated conditions.

		Climate Change Scenario			
		Control x2 Initial SD	**RCP 8.5 Only Mean**	**RCP 8.5 Only SD**	**RCP 8.5 x2 Initial SD**
Genetic Correlation	**None**	499.91 (0.18%)	314.88 (37.04%)	500 (0%)	0.05 (99.99%)
	GSTO	494.24 (1.15 %)	306.26 (38.74%)	500 (0%)	0 (100%)
	TDE	500 (0%)	500 (0%)	500 (0%)	0.93 (99.81%)
	GSTO + TDE	500 (0%)	491.54 (1.69%)	500 (0%)	0.11 (99.97%)

Table S3. Changes in the average value of traits conforming a thermal performance curve and in the average reproductive success across climate change (C.C.), genetic correlations and generations throughout our simulations. For each pairwise combination generations 0, 5 and 85 are shown to indicate change after the acclimatization period and at the end of environmental change. Across all simulations, the initial values for CT_{min}, T_{opt}, CT_{max} and P_{max} were the same and are indicated as "Shared Initial".

			Genetic Correlations (G.C.)				
Trait	**Climate Change Scenario**	**Generation**	**None**	**GSTO**	**TDE**	**GSTO + TDE**	$\overline{\textbf{G.C}}$
CT_{min} (°C)	Shared Initial	0	10	10	10	10	10
	RCP 4.5	5	10	11.1	9.97	10.8	10.47
		85	9.49	11.7	9.82	11.4	10.6
	RCP 6	5	10	11	9.98	10.8	10.45
		85	9.58	11.6	9.79	11.3	10.57
	RCP 8.5	5	10	11	10	10.7	10.43
		85	10.3	11.7	9.79	11.5	10.82
	$\overline{\textbf{RCP}}$	5	10	11.03	9.91	10.76	10.43
		85	9.79	11.67	9.8	11.4	10.66
T_{opt} (°C)	Shared Initial	0	25	25	25	25	25
	RCP 4.5	5	25.6	25.6	26.4	26	25.9
		85	26.3	26.6	27.9	27	26.95
	RCP 6	5	25.7	25.7	26.4	26.1	25.98
		85	26.3	26.6	27.9	27.1	26.98
	RCP 8.5	5	25.7	25.6	26.4	26.1	25.95
		85	26.7	26.8	27.8	27.1	27.1
	$\overline{\textbf{RCP}}$	5	25.67	25.63	26.4	26.06	25.43
		85	26.43	26.67	27.86	27.06	26.8
CT_{max} (°C)	Shared Initial	0	32.5	32.5	32.5	32.5	32.5
	RCP 4.5	5	32.8	31.8	32.6	31.8	32.25
		85	33.6	32	32.7	31.1	32.35
	RCP 6	5	32.8	31.8	32.6	31.9	32.28
		85	33.6	32.1	32.8	32.3	32.7
	RCP 8.5	5	32.8	31.8	32.6	31.9	32.28
		85	34.2	32.6	33.2	32.8	33.2
	$\overline{\textbf{RCP}}$	5	32.8	31.8	32.6	31.86	32.27
		85	33.8	32.23	32.9	32.06	32.75
P_{max}	Shared Initial	0	10	10	10	10	10
	RCP 4.5	5	10.3	11.9	11.1	12.3	11.4
		85	10.7	12.5	12.3	13.6	12.28
	RCP 6	5	10.4	11.9	11.2	12.3	11.45
		85	10.7	12.6	12.3	13.5	12.28
	RCP 8.5	5	10.3	11.9	11.1	12.3	11.4

		85	10.7	12.4	12.2	13.3	12.15
	$\overline{\textbf{RCP}}$	5	10.33	11.9	11.16	12.3	11.42
		85	10.7	12.5	12.26	13.46	12.23
Reproductive Success	**RCP 4.5**	0	4.06	4.43	4.86	4.98	4.58
		5	6.82	10.8	9.68	11.9	9.8
		85	4.48	7.07	11.1	10.1	8.19
	RCP 6	0	4.04	4.39	4.81	4.91	4.54
		5	6.88	10.9	9.68	12	9.87
		85	3.4	5.06	10.1	8.37	6.73
	RCP 8.5	0	4.03	4.44	4.85	4.99	4.58
		5	6.53	10.4	9.45	11.6	9.5
		85	0.7	0.45	1.7	1.07	0.98
	$\overline{\textbf{RCP}}$	0	4.04	4.42	4.84	4.96	4.56
		5	6.74	10.7	9.6	11.83	9.72
		85	2.86	4.19	7.63	6.51	5.29

1014